

Magnetic field intensification by three-dimensional “explosion” process

H. Hotta¹, M. Rempel² and T. Yokoyama¹

¹*Department of Earth and Planetary Science, University of Tokyo, 7-3-1 Hongo, Bunkyo-ku, Tokyo 113-0033, Japan*

²*High Altitude Observatory, National Center for Atmospheric Research, Boulder, CO, USA*

hotta.h@eps.s.u-tokyo.ac.jp

ABSTRACT

We investigate an intensification mechanism for the magnetic field near the base of the solar convection zone that does not rely on differential rotation. Such mechanism in addition to differential rotation has been suggested by studies of flux emergence, which typically require field strength in excess of those provided by differential rotation alone. We study here a process in which potential energy of the superadiabatically stratified convection zone is converted into magnetic energy. This mechanism, known as “explosion of magnetic flux tubes”, has been previously studied in the thin flux tube approximation as well as two-dimensional MHD simulations, we expand the investigation to three-dimensional MHD simulations. Our main result is that enough intensification can be achieved in a three-dimensional magnetic flux sheet as long as the spatial scale of the imposed perturbation normal to the magnetic field is sufficiently large. When this spatial scale is small, the flux sheet tends to rise toward the surface, resulting in a significant decrease of the magnetic field amplification.

Subject headings: Sun: interior — Sun: dynamo — Stars: interiors

1. Introduction

The solar magnetic field is thought to be generated by dynamo action (Parker 1955). In most solar dynamo models differential rotation is the key process that generates strong toroidal field near the base of the convection zone. (Choudhuri et al. 1995; Dikpati & Charbonneau 1999; Hotta & Yokoyama 2010a,b). The mean energy density of dynamo-generated magnetic field is determined by the energy density of differential rotation as:

$$\frac{B^2}{8\pi} \sim \frac{1}{2}\rho(\Delta v)^2, \quad (1)$$

where B , ρ , and Δv denote the strength of magnetic field, density and typical difference of the fluid velocity at the tachocline. At the tachocline these values are $\rho = 0.2 \text{ g cm}^{-3}$, $\Delta v = 2\pi R_{\text{bc}}\Delta\Omega = 2\pi \times 5 \times 10^{10} \text{ cm} \times 50 \text{ nHz} = 15700 \text{ cm s}^{-1}$ (see the results of helioseismology in Thompson et al. 2003), where R_{bc} and $\Delta\Omega$ are the radius at the tachocline and the difference of angular velocity between the top and the bottom of the tachocline, respectively. In addition, if we assume a linear velocity profile and formally integrate that over the width of the shear layer, we have a drop by another factor of 3 in energy. Using these values the dynamo-generated magnetic field is estimated to be approximately $B \sim 1.4 \times 10^4 \text{ G}$. This estimate is similar to the values found in mean-field models with Lorentz force feedback by Rempel (2006). Note that in Rempel (2006) latitudinal shear mostly generates toroidal magnetic field and that differential rotation is continuously replenished through the Λ -effect (parameterized turbulent angular momentum transport), which explains why 10^4 G can be reached with only small feedback on differential rotation.

On the other hand, theoretical studies of flux emergence and their comparison with observed sunspot properties (Joy’s law, low latitude emergence) imply substantially stronger field near the base of the convection zone. Weber et al. (2011) suggest that a toroidal field strength of about 50 kG is required at the base of the convection zone in order to reproduce the statistical properties of tilted sunspot pairs in rising flux tube simulations (see also review by Fan 2009).

Above results suggest that additional mechanisms for the amplification other than rotational shear are required. One candidate of such a mechanism is the “explosion” of rising magnetic flux tubes. (Parker 1994; Moreno-Insertis et al. 1995; Rempel & Schüssler 2001). It is summarized as follows: Suppose that there is a superadiabatically stratified atmosphere like the solar convection zone and a dynamo-generated toroidal magnetic field. When the gravity has the profile of $g(r) \propto r^{-2}$, where r denotes the radius, the distribution of gas pressure $p_e(r)$ is expressed as

$$p_e(r) = p_{\text{base}} \left[1 + \nabla \frac{r_{\text{base}}}{H_{\text{base}}} \left(\frac{r_{\text{base}}}{r} - 1 \right) \right]^{1/\nabla}, \quad (2)$$

using a constant temperature gradient as

$$\nabla \equiv \frac{d \log T}{d \log p}. \quad (3)$$

p_{base} and H_{base} denote the gas pressure and the pressure scale height at $r = r_{\text{base}}$, respectively, where r_{base} is the location of the base of the convection zone. As the toroidal field buoyantly rises as a flux tube, the thermal property in the tube vary adiabatically while the surrounding gas in the convection zone is stratified in a superadiabatic manner. The thermal exchange

is mainly by radiative diffusion in the solar convection zone and the time scale of it is at least several tens of years for a 1000 km flux sheet, which is much longer than the time scale of flux emergence on the order of months. Therefore the internal distribution of the gas pressure is expressed as:

$$p_i(r) = p_{\text{base}} \left[1 + \nabla_{\text{ad}} \frac{r_{\text{base}}}{H_{\text{base}}} \left(\frac{r_{\text{base}}}{r} - 1 \right) \right]^{1/\nabla_{\text{ad}}}, \quad (4)$$

where ∇_{ad} denotes the adiabatic temperature gradient. We note that $\nabla > \nabla_{\text{ad}}$ and the pressure of the internal medium of magnetic flux decreases slower with r than that of the external medium. Suppose that the pressure is in balance at the base of convection zone as:

$$p_i(r_{\text{base}}) + \frac{B^2(r_{\text{base}})}{8\pi} = p_e(r_{\text{base}}). \quad (5)$$

As the decrease of the pressure in the tube is slower than that of the surrounding plasma, these pressures become the same at a certain height $r = r_{\text{expl}}$, i.e., $p_i(r_{\text{expl}}) = p_e(r_{\text{expl}})$. This height is called the explosion height. Even after passing the explosion height, the flux tube continues to rise up to the surface of the sun $r = r_t$. During this process, mass in the flux tube is swept out due to the imbalance between the pressure gradient and the gravitational force along the magnetic field (see Fig. 2 of Rempel & Schüssler 2001). We specify the gas pressure distribution $p_{i,t}(r)$, after this sweeping of mass. Since the gas pressure is balanced at the surface, i.e. $p_{i,t}(r_t) = p_e(r_t)$, the pressure distribution is expressed as:

$$p_{i,t}(r) = p_e(r_t) \left[1 + \nabla_{\text{ad}} \frac{r_t}{H_t} \left(\frac{r_t}{r} - 1 \right) \right]^{1/\nabla_{\text{ad}}}, \quad (6)$$

where a subscript “t” denotes the value at the surface. If both ends of the the rising flux tube stay at the initial position ($r = r_{\text{base}}$), the amplified magnetic field has the energy density of

$$\frac{B_{\text{amp}}^2}{8\pi} = p_e(r_{\text{base}}) - p_{i,t}(r_{\text{base}}), \quad (7)$$

Since the pressure is in balance at the surface with the amplified field, the magnetic field is amplified up to the strength for which the explosion height approaches the surface. The asymptotic field strength is independent of the initial magnetic field and given by the superadiabaticity of the convection zone.

Moreno-Insertis et al. (1995) investigate explosion using one-dimensional thin flux tube approximation. Rempel & Schüssler (2001) show using two-dimensional MHD calculation that magnetic field can be amplified up to 10^5 G in the solar convection zone. The time scale of amplification is determined by the initial magnetic field and is < 0.5 year when the initial plasma beta is $\beta < 10^7$.

In this study, we investigate the possibility of an explosion of a magnetic flux and its consequential intensification by MHD simulations in three-dimensions, i.e. in more realistic situations, which have not yet been investigated in previous studies.

2. Model

The three-dimensional magnetohydrodynamic equations are solved in Cartesian coordinates (x, y, z) , where x and y denote the horizontal directions and z denotes the vertical direction. Equations are expressed as:

$$\frac{\partial \rho}{\partial t} = -\nabla \cdot (\rho \mathbf{v}), \quad (8)$$

$$\frac{\partial}{\partial t} (\rho \mathbf{v}) = -\nabla \cdot \left[\rho \mathbf{v} \mathbf{v} + \left(p + \frac{B^2}{8\pi} \right) \mathbf{I} + \frac{\mathbf{B} \mathbf{B}}{4\pi} \right] - \rho g \mathbf{e}_z, \quad (9)$$

$$\frac{\partial \mathbf{B}}{\partial t} = \nabla \times (\mathbf{v} \times \mathbf{B}), \quad (10)$$

$$\frac{\partial e}{\partial t} = \nabla \cdot \left[\left(e + p + \frac{B^2}{8\pi} \right) \mathbf{v} - (\mathbf{B} \cdot \mathbf{v}) \frac{\mathbf{B}}{4\pi} \right] - \rho g v_z, \quad (11)$$

$$e = \frac{p}{\gamma - 1} + \frac{1}{2} \rho v^2 + \frac{B^2}{8\pi}, \quad (12)$$

where ρ , p , \mathbf{v} , \mathbf{B} , g and e denote density, pressure, fluid velocity, magnetic field, gravitational acceleration, and total energy per unit volume. The value of a specific heat ration is set as $\gamma = 5/3$. Note that since we use the equation of state for the perfect gas, the internal energy per unit volume is expressed as $p/(\gamma - 1)$ in eq. (12)

The divergence free condition, i.e. $\nabla \cdot \mathbf{B} = 0$, is maintained using the method introduced in Dedner et al. (2002). The simulation domain is $(-7.5, -20, -1) < (x/H_b, y/H_b, z/H_b) < (7.5, 20, 3)$ and the total grid number is $256 \times 128 \times 384$. We use a forth-order centered finite difference scheme for spatial-derivatives in combination with a forth-order Runge-Kutta integration in time. We do not use any explicit viscosity or magnetic diffusivity, but apply artificial diffusivities to maintain numerical stability (Rempel et al. 2009). We use periodic boundary conditions for all variables in horizontal directions. At the top and bottom boundary, stress-free and non-penetrating boundary conditions are adopted, i.e. $\partial v_x / \partial z = \partial v_y / \partial z = 0$ and $v_z = 0$. The values of density and pressure at these boundaries are derived from solving eq. (20)-(23). At the top boundary, the magnetic field is set as $B_x = B_y = 0$, and $\partial B_z / \partial z = 0$. At the bottom boundary the magnetic field is set as, $\partial B_x / \partial z = \partial B_y / \partial z = \partial B_z / \partial z = 0$.

The profile of gravitational acceleration is assumed to be

$$g(z) = g_b \left(\frac{z + r_b}{r_b} \right)^2, \quad (13)$$

where $r_b = 5H_b$ is the location of $z = 0$ from the center of the gravity source. We note that the subscript ‘b’ means the value at $z = 0$. Here H_b is used instead of H_{base} since the setup of the simulations here is similar to but not identical with the model in Section 1. The initial magnetic field is set as a flux sheet with a perturbation as:

$$B_x = B_0 f \exp \left[-\frac{(z - z_c)^2}{a^2} \right], \quad (14)$$

$$a = a_0 + a_1 \exp \left[-\left(\frac{x}{d_x} \right)^2 - \left(\frac{y}{d_y} \right)^2 \right], \quad (15)$$

$$z_c = z_0 + z_1 \exp \left[-\left(\frac{x}{d_x} \right)^2 - \left(\frac{y}{d_y} \right)^2 \right], \quad (16)$$

$$f = \frac{a_0}{a}, \quad (17)$$

$$B_0 = \sqrt{\frac{8\pi p_b}{\beta}}, \quad (18)$$

$$(19)$$

where a , and z_c denote the thickness and the center of a flux sheet, respectively. d_x and d_y are the range of perturbation in x and y direction, respectively. We specify $a_0 = 0.2H_b$, $a_1 = 0.25H_b$, $z_0 = 0.1H_b$, $z_1 = 0.25H_b$, $\beta = 300$ and $d_x = 2H_b$. d_y is a free parameter from $2H_b$ to $8H_b$. As shown above, we are considering a toroidal flux sheet as a source of the magnetic flux prior to the intensification because the magnetic field stretched by the Ω -effect at the bottom of the convection zone is suggested to have a sheet structure according to Rempel (2006). Then B_z is calculated to satisfy the divergence free condition, i.e. $\partial B_x/\partial x + \partial B_z/\partial z = 0$ with $B_z = 0$ at the all boundaries and $B_y = 0$ in all the domain.

In order to mimic the situation of the solar convection zone, we adopt a similar approach as Rempel & Schüssler (2001). The upper layer ($z > 0$) is adiabatically stratified (convection zone: $\delta = 0$) and the lower layer ($z < 0$) is subadiabatically stratified (radiative zone: $\delta = -0.2$), where δ is the superadiabaticity. The magnetic layer is placed at the interface between both regions. Since our convection zone is adiabatically stratified we add additional entropy within the flux sheet to allow for a buoyant rise and subsequent explosion. Using this setting, the pressure scale height in the flux sheet is longer than that of the external medium and the explosion occurs around $z_{\text{expl}} \sim H_b c_p / \beta \Delta s$, where Δs is the added entropy. Using an adiabatic stratification in the upper layer allows us to study the explosion process

in a relatively simple situation without thermal convection; this leads, however, also to limitations since some key processes are not captured in our setup. Beside not capturing the influence from convection, our magnetic flux sheet is not stored in stable layer having neutral magnetic buoyancy, i.e. overshoot region at the base of the solar convection zone. The flux sheet is however stabilized against buoyancy to some degree by lying on top of our stably stratified lower layer. We will investigate the explosion process in a superadiabatic convection zone with fully developed thermal convection in a future study.

The initial conditions for pressure and density are derived from solving the equations:

$$\frac{\partial s}{\partial z} = -\frac{c_p \delta}{H_p} - \frac{2\Delta s(z - z_c)}{a^2} \exp\left[-\frac{(z - z_c)^2}{a^2}\right], \quad (20)$$

$$\frac{\partial p_{\text{tot}}}{\partial z} = -\rho g, \quad (21)$$

$$p_{\text{tot}} = p + \frac{B^2}{8\pi}, \quad (22)$$

$$\rho = \left[\frac{p}{\exp(s/c_v)} \right]^{1/\gamma}. \quad (23)$$

We specify $\Delta s = 0.03c_v$. Using this parameter the explosion height is around $z_{\text{expl}} = 0.18H_b$. We do not yet aim at a realistic simulation with solar parameters but rather consider a model that allows us to study the explosion and the following intensification in (artificial) isolation. If there is a superadiabatically stratified convection zone, turbulent thermal convection is generated and the situation becomes more complicated.

3. Result

In this study, we take the y -component of the perturbation on the initial magnetic field (d_y) as a free parameter. Fig. 1 shows the strength and the field lines of the magnetic field for simulations with $d_y = 2H_b$ and $d_y = 6H_b$. We present here only the solutions in the center region cut at $y = 0$ to enhance the clarity of the presentation. The magnetic layer fills in the horizontal directions the whole domain outlined by the white lines. In our three-dimensional situation a value of $d_y = 6H_b$ (Fig. 1d) leads to a substantial intensification of magnetic field, which is similar to the two-dimensional calculation reported by Rempel & Schüssler (2001). At the foot-points the magnetic field lines remain almost parallel to the x -axis for $d_y = 6H_b$. On the other hand, the amplification of magnetic field is significantly less with $d_y = 2H_b$. In the result with $d_y = 2H_b$, the foot-point magnetic field rises upward and the magnetic field lines at the back ($y < 0$) are bent to the center ($y \sim 0$) of the calculation domain. At this stage, it is suggested that the intensification of magnetic field by explosion

process is more likely to occur with a longer perturbation, which is perpendicular to the main magnetic field.

Fig. 2a shows the temporal evolution of magnetic energy averaged over the $y = 0$ plane. Around $t = 120H_b/c_b$, where c_b is the speed of sound at $z = 0$, the initial intensification of magnetic field with explosion process is completed in all cases, i.e. the top of the rising flux is reaching the upper boundary. Fig. 2b shows the dependence on d_y of the mean magnetic energy at $t = 120H_b/c_b$. It is qualitatively clear that a larger scale d_y causes a more effective intensification.

In the following discussion, we compare the results with different d_y at the time when the apex of the rising magnetic flux sheet reaches $z = 2H_b$ in each case. Fig. 2c shows the profile of the y -component of the fluid velocity averaged over $-0.1H_b < x < 0.1H_b$ and $0 < z < 2H_b$ at $y = 0$. Fig 2d shows the dependence of the maximum value of the averaged y -component fluid velocity. The flow parallel to the y -axis is generated by a pressure gradient $\partial p/\partial y$: As the magnetic flux rises, the gas pressure in the central region decreases and it causes a converging flow in the y -direction. The amplitude of the fluid velocity is estimated as $v_y = \tau \Delta p / (\rho d_y)$, where Δp denotes the perturbations of the gas pressure with respect to the ambient medium and τ the time intervall over which the acceleration takes place. For our estimate we use values of $\rho \sim \rho_b$, and $\tau \sim 100H_b/c_b$, The difference of the pressure is estimated to be $\Delta p \sim 0.001p_b$ which is the same order of p_b/β , where ρ_b and p_b are the density and pressure at $z = 0$. Thus we obtain $v_y = 0.1H_b c_b / d_y$. The dashed line in Fig. 2d corresponds to this equation. Overall the result with $d_y = 4H_b, 6H_b, \text{ and } 8H_b$ are well reproduced. The result with $d_y = 2H_b$ is slightly smaller than the value estimated from $v_y = 0.1/d_y$. The reason is that the center region is already filled with mass, resulting in a smaller Δp . In addition, a small value of τ with $d_y = 2H_b$ causes the deviation. Fig. 3a shows the value of v_{perp} along the field lines, where v_{perp} is the fluid velocity perpendicular to the magnetic field in the x - z plane. A positive (negative) value of v_{perp} indicates a flow which moves the magnetic flux upward (downward). Using small (large) d_y , the foot-point magnetic flux move upward (downward). Fig 3b shows the velocity parallel to the magnetic field along magnetic field lines. The larger velocity is generated with larger d_y . These correspond to the amplification of the magnetic field.

4. Discussion

Our results show that the efficiency of the magnetic intensification is dependent on the spatial scale of the perturbations (d_y). The reason is understood as follows: In a two-dimensional situation (Rempel & Schüssler 2001) or using large value of $d_y (> 6H_b)$, the

pressure gradient $\partial p/\partial x$ leads to strong converging flows toward the center of the rising flux sheet within the $y = 0$ -plane. The flow component parallel to the field leads to amplification, the flow component perpendicular to the field prevents the buoyant motion around the legs of the rising flux and consequently plays a role for pinning down the foot-points (Fig. 4a). On the other hand, using small $d_y (< 2H_b)$, a converging motion in the y -direction is promoted by the large pressure gradient $\partial p/\partial y$ and the center of the explosion region is filled with the mass. Thus the pressure around the foot-point becomes large and the flow v_x is suppressed. Consequently magnetic flux moves upward and is less amplified (Fig. 4b). If the foot-point magnetic field is fixed at the initial position, the amplification of magnetic energy is estimated with eq. (7). In a three-dimensional situation, however there is a possibility that the foot-point magnetic flux moves upward, thus the amplified magnetic energy is estimated using eq. (7) at $r = r_f$ instead of $r = r_{\text{base}}$, where r_f denotes the location of the foot-point magnetic flux. Fig. 5 shows the dependence of the amplified magnetic energy by the explosion process on the location of foot-point with the parameters of our calculation. If the foot-point magnetic field is fixed in the initial position, the magnetic energy of $\sim 2 \times 10^{-2} p_b$ can be generated by the explosion process. The result with large $d_y (= 6H_b)$ well reproduces this estimation (see Fig. 1d). Note that Fig. 2a shows the mean magnetic energy in the $y = 0$ plane, leading to a lower values of $\sim 6 \times 10^{-4} p_b$ at maximum. Fig. 5 shows that the efficiency of the intensification significantly decrease as the foot-point magnetic field rises. It is confirmed that even using larger $\beta (= 600)$, we can obtain similar results, i.e. strong amplification is achieved with larger $d_y (> 6H_b)$.

5. Summary

We investigate an intensification mechanism of magnetic field near the base of solar convection zone following the “explosion” process using three-dimensional MHD simulation. Such a mechanism in addition to differential rotation has been suggested by studies of flux emergence, which typically require field strength in excess of those provided by differential rotation alone. Our main result is that the enough intensification can be achieved even in a three-dimensional situation as long as the spatial scale of the imposed perturbation in the direction normal to the magnetic flux sheet is sufficiently large. When this spatial scale is small, the efficiency of intensification of magnetic field significantly decreases. Here a strong converging flow in the direction perpendicular to the field (y -direction) is driven, which leads to weaker flows in the x -direction. The latter are crucial for the field amplification as well as stabilization of the foot-points in our setup.

In this study, we used a similar setup as Rempel & Schüssler (2001), which allows to

study the explosion process in an adiabatically stratified atmosphere, avoiding the complex situation caused by presence of turbulent thermal convection. Using a more realistic setup with a superadiabatic convection zone and storage of magnetic flux in a subadiabatic region beneath could influence our results in the following way:

If the initial magnetic flux is stored in a subadiabatic stratification the foot-point magnetic field is more stable and the criterion for the length scale of the perturbation might be relaxed, i.e. also shorter perturbations could lead to stronger amplification. However, even with more realistic storage in a subadiabatic region, there is no force that could stop the horizontal motion of the foot-points (buoyancy only works in vertical direction). As a consequence also here a fundamental difference between tube-like and sheet-like behavior will persist.

The presence of turbulent thermal convection could significantly influence our results since during the explosion process the strength of magnetic field near the top of the rising flux drops significantly. Thus, it is possible that the connection between top and foot-point magnetic field is disturbed by turbulence, resulting in a reduction of field intensification.

Therefore more realistic simulations including a stably stratified overshoot region/radiation zone and a superadiabatic convection zone are required in order to investigate the detailed conditions under which the explosion process leads to substantial intensification of magnetic field.

The authors are grateful to Y. Fan for her helpful comments. Numerical computations were, in part, carried out on a Cray XT4 at the Center for Computational Astrophysics, CfCA, of the National Astronomical Observatory of Japan. This work was supported by Grant-in-Aid for JSPS Fellows. This work was supported by the JSPS Institutional Program for Young Researcher Overseas Visits and the Research Fellowship from the JSPS for Young Scientists. The National Center for Atmospheric Research is sponsored by the National Science Foundation.

REFERENCES

- Choudhuri, A. R., Schüssler, M., & Dikpati, M. 1995, *A&A*, 303, L29
- Clyne, J., Mininni, P., Norton, A., & Rast, M. 2007, *New J. Phys*, 9
- Clyne, J., & Rast, M. 2005, in *Proceedings of Visualization and Data Analysis 2005*

- Dedner, A., Kemm, F., Kröner, D., Munz, C.-D., Schnitzer, T., & Wesenberg, M. 2002, *Journal of Computational Physics*, 175, 645
- Dikpati, M., & Charbonneau, P. 1999, *ApJ*, 518, 508
- Fan, Y. 2009, *Living Reviews in Solar Physics*, 6, 4
- Hotta, H., & Yokoyama, T. 2010a, *ApJ*, 709, 1009
- . 2010b, *ApJ*, 714, L308
- Moreno-Insertis, F., Caligari, P., & Schüssler, M. 1995, *ApJ*, 452, 894
- Parker, E. N. 1955, *ApJ*, 122, 293
- . 1994, *ApJ*, 433, 867
- Rempel, M. 2006, *ApJ*, 647, 662
- Rempel, M., & Schüssler, M. 2001, *ApJ*, 552, L171
- Rempel, M., Schüssler, M., & Knölker, M. 2009, *ApJ*, 691, 640
- Thompson, M. J., Christensen-Dalsgaard, J., Miesch, M. S., & Toomre, J. 2003, *ARA&A*, 41, 599
- Weber, M. A., Fan, Y., & Miesch, M. S. 2011, *ApJ*, 741, 11

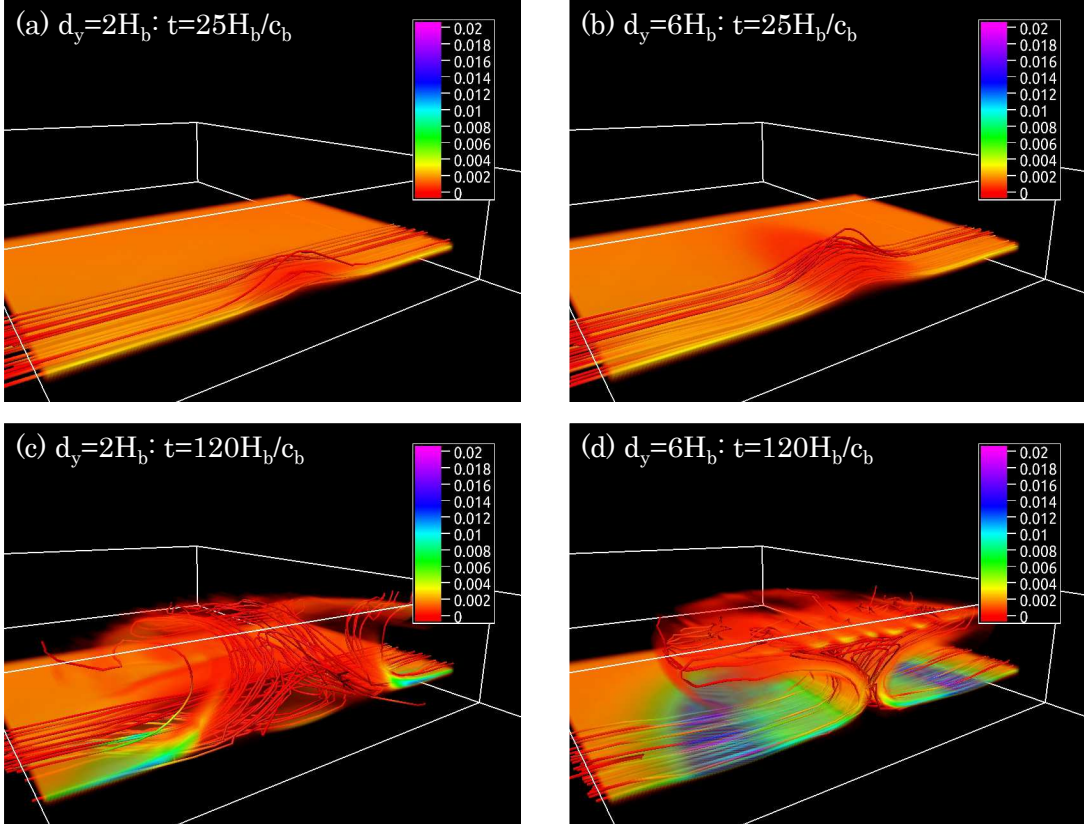


Fig. 1.— The volume-rendered magnetic energy and the magnetic field lines. The panels a and c (b and d) show the results with $d_y = 2H_b$ ($d_y = 6b$). For convenience of presentation, we show only the solution in the center region cut at $y = 0$. The color shows the magnetic energy normalized by the gas pressure at $z = 0$ (p_b). This visualization is created using the software of VAPOR (Clyne & Rast 2005; Clyne et al. 2007).

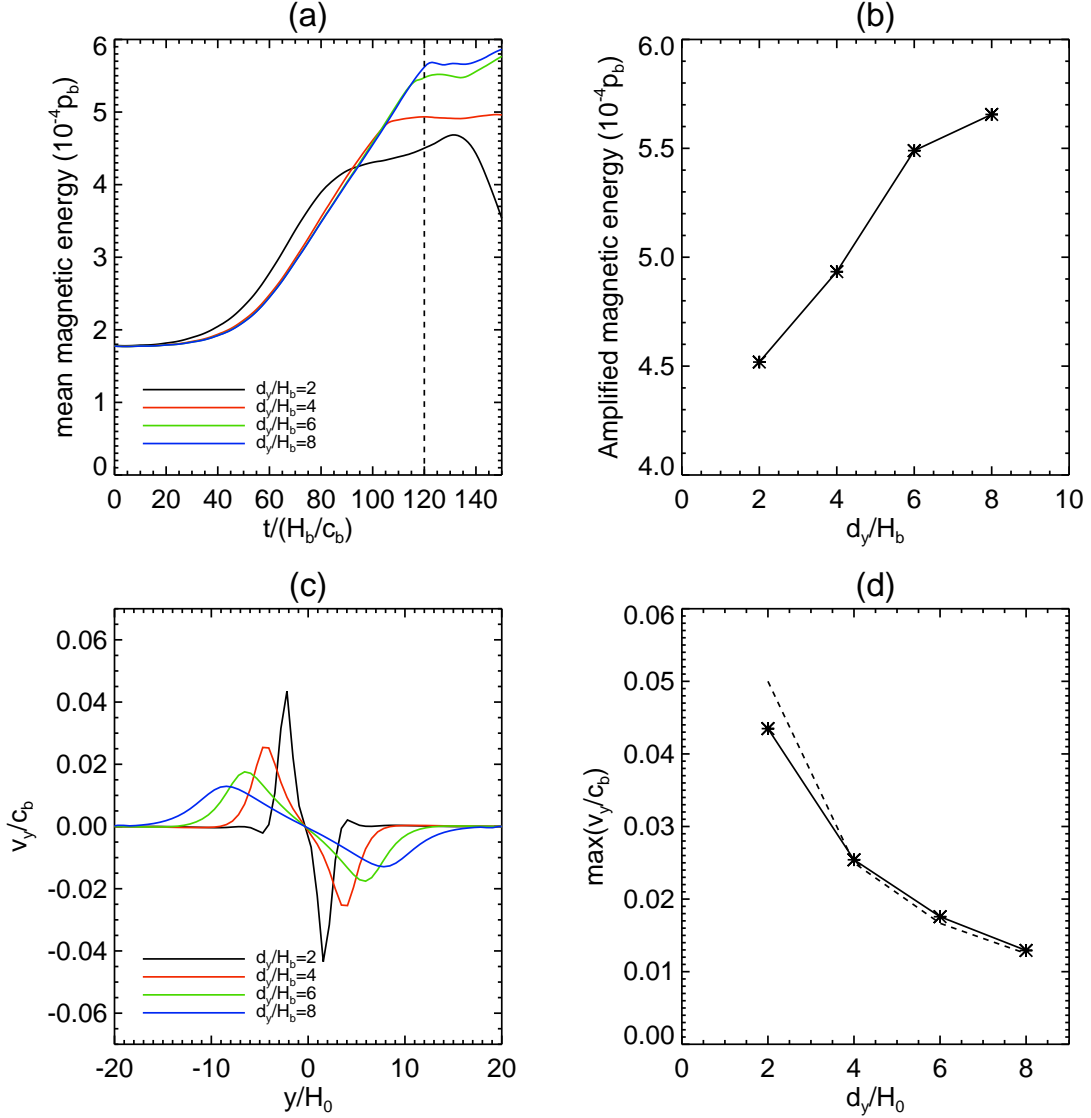


Fig. 2.— (a) Temporal evolution of the mean magnetic energy $|B^2/8\pi|$ on the $y = 0$ plane. (b) The dependence of the mean magnetic energy at $t = 120H_b/c_b$ on d_y . The energy of magnetic field is normalized by $10^{-4}p_b$. (c) The profile of y -component fluid velocity averaged over $-0.1H_b < x < 0.1H_b$ and $0 < z < 2H_b$ at $y = 0$. (d) The dependence of the maximum value of the averaged y -component velocity on d_y . The dashed line denotes the dependence of $v_y = 0.1/d_y$.

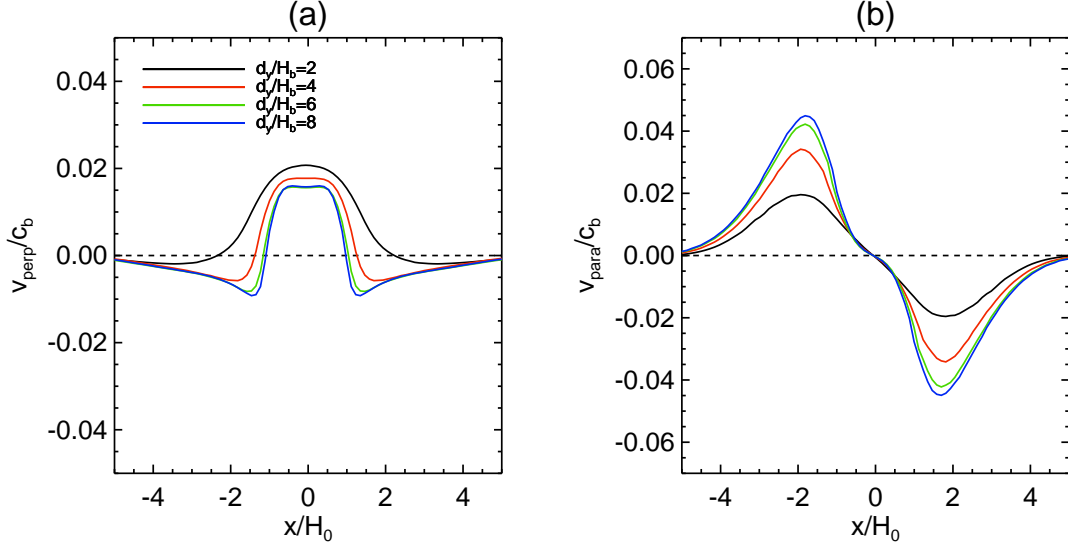


Fig. 3.— (a) Averaged v_{perp} along magnetic field lines, where v_{perp} is the fluid speed perpendicular to the magnetic field. We choose the magnetic field lines which start $x = y = 0$ and $z = 0, 0.25H_b$. (b) Averaged velocity parallel to magnetic field v_{para} is shown. The same magnetic field lines for the panel (a) are chosen.

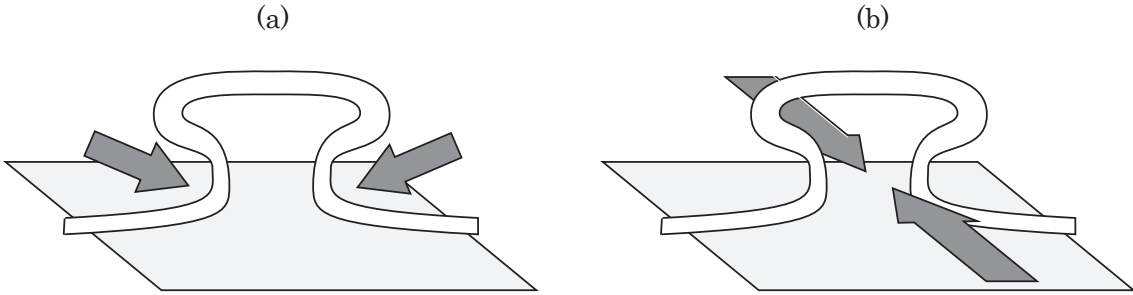


Fig. 4.— Schematic picture of the explosion process in three-dimensional situation with (a) large and (b) small d_y .

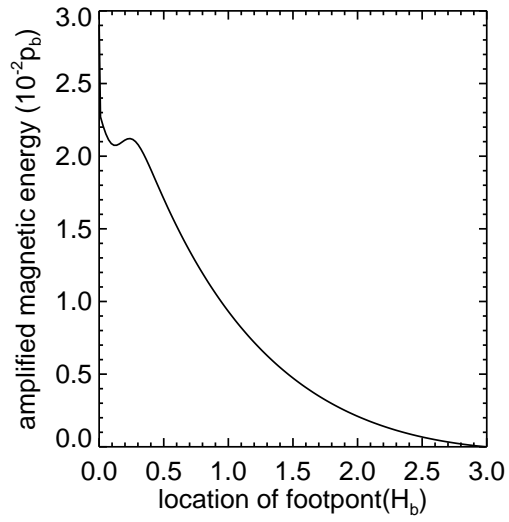


Fig. 5.— The dependence of the amplified magnetic energy by the explosion process on the location of foot-point.